Studies of domain wall motion. II. Models of the dynamic internal friction

1991 J. Phys.: Condens. Matter 3 4783

(http://iopscience.iop.org/0953-8984/3/26/002)

J. Phys.: Condens. Matter 3 (1991) 4783–4795. Printed in the UK

Studies of domain wall motion: II. Models of the dynamic internal friction

W G Zeng†, J X Zhang† and G G Siu‡

† Department of Physics, Zhongshan University, Guangzhou, People's Republic of China

‡ Department of Applied Science, City Polytechnic of Hong Kong, Hong Kong

Received 23 January 1990, in final form 4 March 1991

Abstract. An interaction model of the motion equation of a domain wall (DW) is used to calculate the DW velocity and hence the internal friction (IF). A magnetomechanical interaction is proposed to explain the dynamic IF and the unique behaviour that the dynamic IF increases with $\dot{H}/\omega$. The model shows that the dynamic IF is not caused by relaxation of DWs and is related to the average velocity of moving DWs. Furthermore, a phenomenological model is proposed and a two-term parametrization expression is used to fit the experimental data of the dynamic IF of Fe, Ni and Permalloy satisfactorily. It is based on the assumption that the superposition of all contributions of magnetic objects (MOs) (a MO is a single equivalent object in terms of the dynamic properties due to correlation between a group of DWs) gives the field dependence of the dynamic IF. Preliminary discussion of the physical meaning of the parameters is given.

Introduction

Low-frequency anelastic studies of soft ferromagnetic materials Fe, Ni and Permalloy-42 using uniform magnetic field sweeping (Zeng *et al* 1990, hereafter referred to as I) show that their internal friction (IF) is divided into static IF and dynamic IF. The static IF Q_0^{-1} has already been studied extensively. Characterized by the variation in damping WRT the amplitude and frequency ω of the strain and by the appearance of an internal peak, Q_0^{-1}(Fe) behaves differently from Q_0^{-1}(Ni), and Q_0^{-1}(Permalloy) lies in between. Essentially, Q_0^{-1}(Fe) is due to the micro-eddy current type of loss at low frequencies, which is similar to the low-frequency branch of the IF of resonance type. In contrast, Q_0^{-1}(Ni) is partially of the static hysteresis type. The cubic solid solution of Fe and Ni—Permalloy—has a behaviour in between those of Fe and Ni. On the other hand, the dynamic IF values Q_m^{-1} for Fe, Ni and Permalloy have the same characteristics: Q_m^{-1} increases with increasing $\dot{H}/\omega$ but its peak position only shifts slightly. The dynamic IF associated with the uniform magnetic field sweeping is caused by the viscoelastic motion of domain walls (DWs) in magnetization, based on its characteristics and its similarity to those of the crystal plastic deformation (Zhang 1981) and NiTi shape memory alloy (Lin *et al* 1989) associated with the motions of dislocations and phase interface, respectively.

Under a constant magnetic field, the equilibrium positions of DWs are shifted to new positions, and DWs oscillate about these new equilibrium positions on application of an alternating stress. It is assumed (Degauque and Astié 1980) that irreversible DW jumps over peaks of the force field are the only cause of magneto-mechanical damping. In

0953-8984/91/264783 + 13 $03.50

magnetic field sweeping, the equilibrium position is always shifting, DWs keep on moving if possible and their mobility is enhanced. It is this DW motion in excess of the former motion which causes the dynamic IF. The purpose of this work is to explain the characteristics of Q_m^{-1} based on the motion equation of DWs per unit area and by proposing a coupled force between the field sweep and applied stress. Although the behaviour of the dynamic IF can be represented by this interaction model, its field dependence has to be interpreted. Hence, we propose a phenomenological model to fit the Q_m^{-1} versus H data of Fe, Ni and Permalloy. The parametrization expression works satisfactorily.

2. An interaction model of the wall motion equation: the magnetomechanical force

On application of a magnetic field, DWs will move under various forces, which are of a driving or restoring type and may originate from magnetostatic, magnetoelastic or wall energy. The DW motion may be discussed in terms of the variation in a single energy E with wall position x, where E stands for any or all of the various above-mentioned energies. It is expected that E will be a randomly varying function of position x owing to the effect of crystal imperfections such as inclusion and residual stress. Although we are ignorant of the exact form of the E versus x curve and the magnetic property of a real specimen is the sum of the results obtained from discussion of this kind of local motion, qualitative understanding may be obtained in many magnetic problems (see, e.g., Cullity 1972). Suppose that, when $H = 0$, a DW is initially located at a potential energy minimum of the E versus x curve. Then the equation of motion of the wall per unit area is

$$\rho(d^2x/dt^2) + \gamma(dx/dt) + \kappa x = G \tag{1a}$$

where ρ is the effective mass density, γ is the damping coefficient, κ is the coefficient of restoring force determined by interactions between DWs and between a DW and crystal defects, and G is the force exerted on DWs per unit area. When a weak field is applied, most walls make a reversible damped motion or tend to make an irreversible motion. In the following, we investigate various driving forces exerted on DWs and then solve the differential equation. It leads to expressions for the static IF and dynamic IF. The results are compared with experiments.

For a cylindrical specimen of annealed polycrystalline pure ferromagnetic material under a low axial magnetizing field $H = \dot{H}t$, the moving walls maintain their planes. We assume that the periodic stress in measuring the IF is along the same axis for simplicity. The stress varies sinusoidally; its amplitude is small and its frequency is in the range 10^{-1}–10 Hz (figure 1). The results obtained for the axial stress are also applicable to our torsion pendulum experiment. In fact, the assumption of axial stress is not necessary for a polycrystalline specimen where DWs orient randomly. The same results can be obtained for a stress which makes an angle of 45° with the axis. In our torsion pendulum experiment, the stress distribution is not so simple but its amplitude can be taken as distributed uniformly along the radial direction for the polycrystalline specimen. The maximum positive stress is equal to shear stress and makes an angle of 45° with the axis based on solid-mechanics analysis. Hence, it leads to the same results.

The orientation of the saturation magnetization vectors M is considered only as a modification of a constant coefficient in the following calculations. In figure 1, θ is the angle between the external magnetic field and M and its values distribute randomly in a polycrystalline specimen. The average of the direction factor $\cos^2\theta$ or $|\cos\theta|$ is $\frac{1}{3}$ or $\frac{1}{2}$

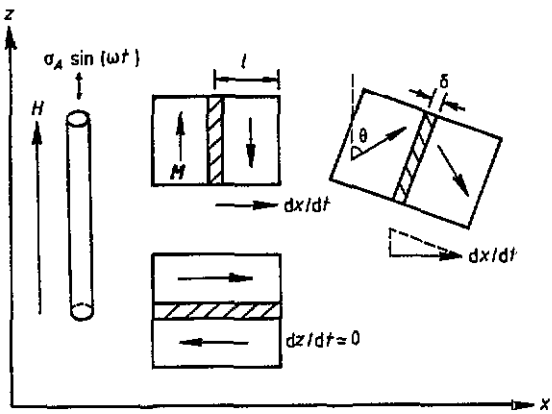

Figure 1. Schematic illustration of DW motion under a uniformly increasing magnetic field and an oscillating stress ($|M| = M_s$).

and only affects a constant coefficient. Also, according to the direction of the external magnetic field and stress, dx/dt is equivalent to dy/dt and $dz/dt \ll dx/dt$ or dy/dt. We shall calculate dx/dt in this mathematical model following Kittel and Galt (1956).

The driving force exerted on walls per unit area includes the following forces.

(i) *The principal driving force* $G_H = A_1^0 \dot{H}t$, where $A_1^0 = a\mu_0 \cos\theta M_s$ and a is a constant ($a = 1$ for 90° wall or 2 for 180° wall), $\dot{H}$ is the constant rate of increase in $H(<100\ \text{mOe s}^{-1})$. Furthermore, let $a_1 = a\mu_0 \cos\theta$ to absorb the effect of the angle θ.

(ii) *The perturbing alternating force* $G_\sigma = A_3^0 \sin(\omega t)$, which is caused by the alternating stress through magnetostriction on a DW. A_3^0 is the amplitude which is the product of the applied stress amplitude σ_A and a coupling factor, which is taken as unity at the beginning so that $A_3^0 = \sigma_A$.

(iii) *The magnetomechanical interaction* $G_a = A_2^0 t \sin(\omega t)$, where $A_2^0 = a_2 \dot{H} A_3^0$ and a_2 is the coefficient of coupling between the magnetic field and the mechanical stress and is determined by material properties. In our wire samples, the demagnetizing field can be ignored. Without external influences, DWs are located in their equilibrium position and their motion will be hindered by the crystalline anisotropy field and internal stress field of the material. Both are affected by the external magnetic and stress fields, i.e. the equilibrium positions and energies of DWs are changed (Cullity 1972). On the other hand, these two external fields themselves interact with each other. Thus, the magnetomechanical interaction is an overall effect resulting from the coupling of external fields with intrinsic properties. This interaction is proposed to take the form of a simple product of force (i) and (ii).

(iv) *The loading time of the alternating stress* is taken as $t = 0$. As a result, the times in (i) and (iii) should be replaced by $t + t_{0i}$ where t_{0i} is the elapsed time of the magnetic field action when the ith periodic stress is applied. An extra force hence arises: $A_0^0 = (A_1^0 \dot{H} + A_2^0) t_{0i}$.

The equation of motion of DWs per unit area describes the movement of the DW oscillation under force (ii) and (iii) under the principal driving force and takes the form

$$\rho(d^2x/dt^2) + \gamma(dx/dt) + \kappa x = A_0^0 + A_1^0 \dot{H}t + A_2^0 t \sin(\omega t) + A_3^0 \sin(\omega t). \qquad (1b)$$

The equation of motion of DWs per unit effective-mass density is

$$d^2x/dt^2 + 2n(dx/dt) + p^2x = A_0 + A_1\dot{H}t + A_2 t\sin(\omega t) + \sigma_m \sin\omega t \tag{2}$$

where

$$2n = \gamma/\rho \qquad p^2 = \kappa/\rho \qquad A_0 = A_0^0/\rho \qquad A_1 = A_1^0/\rho = (a_1/\rho)M_s$$

$$\sigma_m = A_3^0/\rho \qquad A_2 = A_2^0/\rho = a_2\dot{H}\sigma_m.$$

Let $p_d^2 = p^2 - n^2$ and let us present the solution of equation (2) as $x = x_0 + x_1 + x_2 + x_3 + x_4$. It is obtained by the Duhamel integration method.

(i) x_0 corresponds to a free damped oscillation:

$$x_0 = \exp(-nt)\{x_{0i}\cos(p_d t) + [(\dot{x}_{0i} + nx_{0i})/p_d]\sin(p_d t)\}. \tag{3}$$

(ii) x_1 is due to the external magnetic field force applied at the same time as the alternating stress:

$$x_1 = (A_1\dot{H}/p^2)(t - 2n/p^2) + (A_1\dot{H}/p^4 p_d)\exp(-nt)\,[2np_d\cos(p_d t) - (p_d^2 - n^2)\sin(p_d t)]. \tag{4}$$

(iii) x_2 is caused by the magnetomechanical interaction applied at the same time as the alternating stress:

$$\begin{aligned} x_2 = {} & (A_2 t/A_3)[(p^2 - \omega^2)\sin(\omega t) - 2n\omega\cos(\omega t)] \\ & + (2A_2/A_3^2)\{n(3\omega^4 - p^4 - 2p^2\omega^2 + 4n^2\omega^2)\sin(\omega t) \\ & - \omega[(p^2 - \omega^2)^2 - 4n^2p^2]\cos(\omega t)\} \\ & + (2A_2\omega/A_3^2)\exp(-nt)\{[(p^2 - \omega^2)^2 - 4n^2p^2]\cos(p_d t) \\ & + (n/p_d)[3p^4 - \omega^4 - 2p^2\omega^2 - 4n^2p^2]\sin(p_d t)\} \end{aligned} \tag{5}$$

where $A_3 = [(p^2 - \omega^2)^2 + 4n^2\omega^2]$.

(iv) x_3 originates in the periodic stress used in measurements:

$$\begin{aligned} x_3 = {} & A_4\cos(\omega t) + A_5\sin(\omega t) - \{A_4[\cos(p_d t) + (n/p_d)\sin(p_d t)] \\ & + (A_5\omega/p_d)\sin(p_d t)\}\exp(-nt) \end{aligned} \tag{6}$$

where $A_4 = (-2n\omega\sigma_m)/A_3$, $A_5 = (p^2 - \omega^2)\sigma_m/A_3$.

(v) x_4 corresponds to A_0 owing to the different times of application of (i) and (ii):

$$\begin{aligned} x_4 = {} & [(A_1\dot{H} + A_2)/p^2]t_{0i} - [(A_1\dot{H} + A_2)/p^2]t_{0i} \\ & \times \exp(-nt)[\cos(p_d t) + (n/p_d)\sin(p_d t)]. \end{aligned} \tag{7}$$

It should be noted that x_i ($i = 1, 2, 3, 4$) satisfy $x_i = 0$ and $\dot{x}_i = 0$ at $t = 0$. Hence, the initial conditions can be chosen as $x_{0i} = 0$ and $\dot{x}_{0i} =$ constant at $t = 0$.

Polycrystalline ferromagnetic materials usually have $p^2 \gg 4n^2$ (Peking University 1976) and, for low-frequency fields, $p^2 \gg \omega^2$, which is very different from the results of O'Dell (1981) due to the difference in materials and experimental conditions, e.g. a pulse rather than an alternating perturbation was used. Hence, the contributions of the steady state (without the term $\exp(-nt)$) in equations (3)–(7) to the IF dominate those of the transient state. The latter will be shown to be negligible by detailed calculations of IF. Also, the term for the steady state in equation (7) does not contribute to the IF, this shows that t_{0i} can be neglected. In the following, only the contributions from the steady state are presented.

The steady-state velocity of DWs is obtained from equations (3)–(7):

$$\begin{aligned} dx/dt = {} & A_1\dot{H}/p^2 + (A_2/A_3)\{[(p^2-\omega^2)\sin(\omega t) - 2n\omega\cos(\omega t)] \\ & + [2n\omega^2 t\sin(\omega t) - \omega(p^2-\omega^2)t\cos(\omega t)]\} \\ & + (2A_2/A_3^2)\{\omega^2[(p^2-\omega^2)^2 - 4n^2p^2]\sin(\omega t) \\ & + n\omega[3\omega^4 - p^4 - 2p^2\omega^2 + 4n^2\omega^2]\cos(\omega t)\} \\ & + [A_5\omega\cos(\omega t) - A_4\omega\sin(\omega t)]. \end{aligned} \tag{8}$$

Based on the IF formula (Ké and Zhang 1975) and considering that equation (2) is the equation of unit effective-mass density, the IF is obtained:

$$Q^{-1} = \frac{\int_0^T \sigma_A \sin(\omega t)\dfrac{dx}{dt}\,dt/2\pi^2\sigma_A^2}{E'} = Q_0^{-1} + Q_m^{-1} \tag{9a}$$

where E' is an appropriate modulus per unit effective-mass density ($E' = E/\rho$) so that σ_A reappeared, and the principal terms of Q_0^{-1} and Q_m^{-1} are

$$Q_0^{-1} = 2n\omega E/p^4[(1-\omega^2/p^2)^2 + 4n^2\omega^2/p^4] \simeq 2n\omega E'/p^4 \equiv \gamma\omega E/\kappa^2 \tag{9b}$$

$$Q_m^{-1} = (a_2 E\dot{H}/p^2\omega)(1 + 2\omega^2/p^2 + 8\pi^2 n\omega/p^2)] \simeq a_2 E'\dot{H}/p^2\omega \equiv a_2 E\dot{H}/\kappa\omega. \tag{9c}$$

In equations (9*b*) and (9*c*), E is the modulus in the usual sense with γ and κ, and E' is taken as the modulus per unit effective-mass density with $2n$ and p^2. The dimensions were checked so that $2n\omega/p^2$, E'/p^2, etc, were found to be dimensionless. It can be seen that Q_m^{-1} results from the magnetomechanical interaction $A_2 t\sin(\omega t)$.

The factor p^2 of the restoring force is different in reversible DW migration from that in irreversible DW migration. Therefore we make a transfomation of equation (9*c*). The magnetization M can be expressed as $M_s x/l$, where l is the distance of the DW equilibrium position from the crystal surface (figure 1) and

$$dM/dt = (M_s/l)(dx/dt). \tag{10a}$$

The average dx/dt over one period under the approximation $p^2 \gg 4n^2$ and $p^2 \gg \omega^2$ is

$$(A_1\dot{H}/p^2)[1 - (2n\omega/p^2)(A_2/A_1\dot{H})] \tag{10b}$$

and it is substituted into the average of equation (10*a*). Since $(2n\omega/p^2)\,(A2/A_1\dot{H}) \ll 1$ according to the above analysis, the second term in equation (10*b*) is negligible and we obtain from equation (10*a*)

$$E'/p^2 = (E'\rho/a_1)(l/M_s^2)(dM/dH). \tag{10c}$$

At a given magnetic field H, the dynamic IF Q_m^{-1} is

$$Q_m^{-1} = (a_2 l/a_1)(E\dot{H}/M_s^2\omega)(dM/dH) \tag{11}$$

and the variation in $1/p^2$ WRT the magnetic field H has been transformed into that of dM/dH.

The results of equations (9) and (11) show that the IF can be divided into two parts: the static IF Q_0^{-1} and the dynamic IF Q_m^{-1}. The static IF is independent of the stress amplitude and magnetic field but proportional to the angular frequency, which is of a micro-eddy current type as Q_0^{-1}(Fe). The dynamic IF Q_m^{-1} exists only on field sweeping

($\dot{H} \neq 0$) and is proportional to $\dot{H}/\omega$. Hence, equation (1) for the motion of DWs per unit area is in general consistent with the experimental results presented in I. Furthermore, equation (11) shows that the dynamic IF is connected with the differential susceptibility and they behave similarly at constant $\dot{H}/\omega$.

An estimate of the order of magnitude of p^2 (or κ) can show that the results are consistent with the approximation $p^2 \gg 2n$. From equation (10*c*) and $p^2 = \kappa/\rho$, it is readily shown that $\kappa = a_1 M_s^2/\chi l$. χ can be approximated by $\mu_r = 1 + \chi \simeq \chi$. Based on the data given by Cullity (1972) and Peking University (1976), $\chi/\mu_0 \simeq 10^3$–10^4, $M_s \simeq 10^4$ G, $l \simeq 10^{-6}$–10^{-5} m when the Fe crystallite size is about 0.024 mm, and $a_1/\mu_0 \simeq 1$. Hence, κ is estimated to be about 10^7–10^8 N m^2 (the DW density is in kilograms per square metre). From equation (9*b*) and taking $Q_0^{-1} \simeq 10^{-3}$, $E \simeq 10^{11}$ N m^{-2}, γ is estimated to be about 10^{-1} N s m^{-2}. These values satisfy $\kappa \gg \gamma$ or $p^2 \gg 2n$.

The contributions of the transient states to IF can be obtained using the same method:

$$Q_{0i}^{-1} = E\omega\dot{x}_{0i}/\pi p^2\sigma_m - (2n\omega/p^4)[n\dot{x}_{0i} - (A_1\dot{H} + A_2)t_{0i}]E/\pi\sigma_m. \tag{9d}$$

On the basis of the values chosen for constants and from experimental conditions for Fe, we have $Q_{0i}^{-1} \simeq 0.1\dot{x}_{0i} - 10^{-8}\dot{x}_{0i} + 10^{-9}t_{0i}$ where $\dot{x}_{0i}$(Fe) $\simeq 10^{-7}$ m s^{-1} and $t_{0i} \simeq 100$ s. Hence, Q_0^{-1} is negligible. However, Q_{0i}^{-1} reflects the IF which depends on the stress amplitude and frequency, and the sweeping magnetic field. For Ni, the contributions of the transient states may be more important because of a larger velocity $\dot{x}_{0i}$(Ni).

These estimates confirm the appropriateness of the approximations made in the derivation of equations (9) and (11). For Fe, they work well but we have to consider the contributions of the transient states for Ni and Permalloy when interpreting the behaviour of their Q_0^{-1}. On the other hand, the dynamic IF is essentially in good agreement with the experimental data given in I. Equation (11) can provide further interpretation for the Q_m^{-1} behaviour of these soft ferromagnetic materials. For example, Q_m^{-1}(Ni) > Q_m^{-1}(Permalloy) since M_s(Ni) < M_s(Permalloy) according to equation (11). Also, equation (11) provides the relationship between Q_m^{-1} and the average (over a period) $\mathrm{d}M/\mathrm{d}H$ as a function of H.

Further studies show, however, that the interaction model needs to be improved. The theoretical result of equation (11) predicts that Q_m^{-1} is proportional to $\dot{H}/\omega$ but the experimentally measured Q_m^{-1} is proportional to $(\dot{H}/\omega)^{s'}$ where s' depends on the value of the magnetic field. The fitted values of s'(Fe) are 0.72, 0.62, 0.53, 0.44 and 0.39 for H = 1 Oe, 2 Oe, 3 Oe, 4 Oe and 5 Oe respectively and all are smaller than 1 (average 0.54). Moreover, the slopes of the curves of ln Q_m^{-1} versus $\dot{H}$ and ln Q_m^{-1} versus ω^{-1} are different. Hence, the relationship between Q_m^{-1} and $\dot{H}/\omega$ is not as simple as shown in equation (11) and the $\dot{H}$-dependence of the dynamic IF is also different from the ω^{-1}-dependence. The coupling factor, which is implicit in A_3^0 and represents coupling of the applied stress onto DWs, in fact, should be frequency dependent. We suggest that the coupling factor takes an explicit form $\sqrt{k}(\omega/\omega_0)^{-\alpha}$, where ω_0 is taken as 1 Hz; α is a rate-sensitive index and k a constant. It follows that the coupling factor will appear in A_2. The same factor is also added in the numerator of equation (9*a*). On the other hand, we replace the term $\dot{H}t$ by a more general term $(\dot{H}t)^s$, which is assumed to include the effect of static friction to DW motion. The effect of the static friction is assumed to be proportional to $(\dot{H}t/H_0)^{s-1}$ where H_0 = 1 mOe so that s is dimensionless. After making these modifications, we obtain

$$Q_m^{-1} = (a_2 l/a_1)(kE/M_s^2)(\mathrm{d}M/\mathrm{d}H)(\dot{H}^s/\omega^{1+s-2\alpha}) \tag{11*}$$

$$Q_0^{-1} = (k\gamma E/\kappa^2)\omega^{1-2\alpha}. \tag{9*}$$

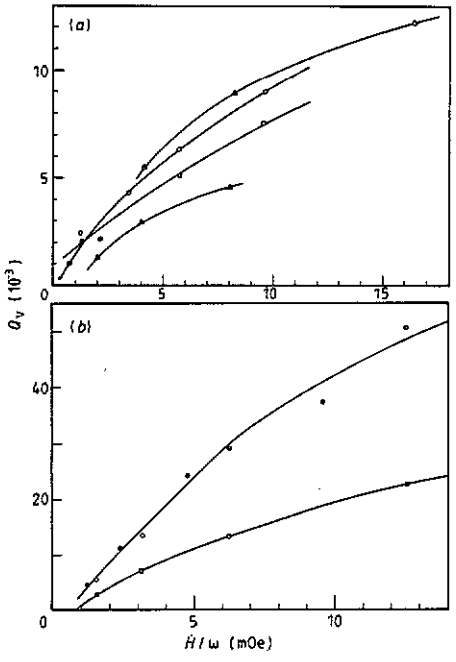

Figure 2. The total dissipated dynamic energy Q_V versus $\dot{H}/\omega$ (*a*) of Fe and Permalloy (○, for annealed Fe at $f = 1.100$ Hz; ●, for annealed Fe at $f = 1.600$ Hz; □, for pre-strained Fe at $f = 1.100$ Hz; △, for annealed Permalloy at $f = 0.773$ Hz; ▲ for annealed Permalloy at $f = 1.586$ Hz) and (*b*) of Ni (○, for annealed Ni at $f = 1.013$ Hz; ●, for annealed Ni at $f = 1.330$ Hz; □, for pre-strained Ni at $f = 1.014$ Hz).

For the comparison with experiments, we need to know the differential susceptibility dM/dH as a function of H, which is studied in the next section.

3. Parametrization of the dynamic internal friction Q_m^{-1}

In the calculations in section 2, the time integral in equation (9*a*) makes it unsuitable for interpreting the field dependence (and hence the time dependence) of Q_m^{-1}. A phenomenological model is needed to provide a meeting point between experimental results and theoretical studies by sorting out the data of Q_m^{-1} versus H for Fe, Ni and Permalloy.

The average grain sizes of the polycrystalline specimens are about 0.024 mm, 0.50 mm and 0.05 mm for pure iron, nickel and Permalloy respectively. For these innumerable DWs the statistical average is inevitably necessary to provide interpretation of the observed results. We hence adopt a treatment based on statistical concepts. The correlation between DWs is not negligible and therefore the fundamental objects providing coherent magnetization changes along the length of the wire specimen are groups of neighbouring DWs. Each group of DWs has a correlation region with a size equal to the wire cross section and can be treated in terms of the dynamic properties as a single equivalent object, a 'magnetic object' (MO) (Bertotti 1987). Each MO contributes independently and a superposition of these contributions gives an interpretation of the DW structure evolution. It is assumed that all MOs follow the same motion equation and, in the following discussion, a DW is used in the sense of a MO.

Table 1. The coefficients of the polynomial $Q_0^{-1} = aH^3 + bH^2 + cH + d$.

Sample	Frequency (Hz)	$a \times 10^6$ (Oe^{-3})	$b \times 10^5$ (Oe^{-2})	$c \times 10^5$ (Oe^{-1})	$d \times 10^4$
Fe	1.100				22.63
Fe	1.600				26.00
Prestrained Fe	1.100				22.83
Ni	1.013	11.70	−29.90	190.86	17.15
Ni	1.330	3.860	−12.20	94.20	13.08
Pre-strained Ni	1.014	−0.3059	0.3484	−0.7420	6.208
Permalloy	0.773	−2.400	1.910	−1.310	8.748
Permalloy	1.568	0.8470	−3.062	19.14	12.38

Equation (9*a*) shows that the increase in DW mobility, i.e. an increase in $\dot{x}$, in general, will enhance the dynamic IF. Equation (11) shows that at constant $\dot{H}$ and ω, Q_m^{-1} is proportional to the differential susceptibility dM/dH. Hence, the H-dependence of Q_m^{-1} is reduced to the H-dependence of dM/dH, which not only reflects the mobility of DWs but also depends on the number of moving DWs. The DW motion concerned in the dynamic IF is the motion caused by the magnetomechanical interaction, which is in excess to the motion of the irreversible jump over peaks of the force field on application of an oscillating stress only (I). In the following, we refer to this motion only. Besides the solution x_2 obtained in equation (5) based on the motion equation, we know little about it. A phenomenological model has to consider the contributions of all moving DWs to dM/dH. It is noticed that the field sweeping, although slow, results in a field region ΔH around H ($H - \Delta H/2$ to $H + \Delta H/2$) in the IF measurements. In this field region, the MO motion under the low-speed compound field is time dependent in a complicated manner owing to the different energy states of the MOS determined by various factors, e.g. the distribution of internal stress and defects. The MOS start, continue or stop moving at different instants. The stopping process is inevitable because of the finite size of the cross section of the wire, because of the defect pinning, because of recombination and disappearance etc. In the field region ΔH around H, the DWs which have newly started and continue to move contribute positively to dM/dH but contributions from the stopped DWs have to be subtracted from the total contributions. If the moving and stopping mechanisms are similar, only the total number of the moving DWs will be meaningful. However, if these mechanisms in the magnetomechanical motion are different, the subtraction of two terms will be inevitable. In the present situation for which we do not know the detailed microscopic description, we can make a general proposal that a parametrization form of the difference of two terms, each of which assumes the form of time exponent (and hence the field H), is employed. The parametrization expression for the dynamic IF is assumed to be as follows:

$$Q_m^{-1} = c_1 \exp(-b_1 H) - c_2 \exp(-b_2 H) \tag{12}$$

where c_1, c_2, b_1 and b_2 are four parameters.

To fit the data of Q_m^{-1}, the Q_0^{-1} versus H curves are fitted first by polynomials $Q_0^{-1} = aH^3 + bH^2 + cH + d$ using software MATLAB and the results are listed in table 1. The fitted curves of Q_0^{-1} are drawn as full curves in figures 3–5 of I. By subtracting Q_0^{-1} from the total IF Q^{-1} at non-zero-field sweep ($\dot{H} \neq 0$), we obtain the dynamic IF

Q_m^{-1}. The data for the dynamic IF obtained in this way for Fe, Ni and Permalloy-42 are fitted to the four-parameter expression (12) using the software MATLAB and the fitted values are shown in table 2. The fitting is carried out in a field region from 0.2 to 6.5 Oe for Fe and Ni, and from 1 to 8 Oe for Permalloy-42. Fields of 0.2 Oe for Fe and Ni and 1 Oe for Permalloy are the lowest for the measurement of IF in swept field so that we can take these as the effective zero points of field for the dynamic IF. The total IF as the sum of Q_0^{-1} and Q_m^{-1} through fitting are presented by full curves in the cases of $\dot{H} \neq 0$ in figures 3–5 of I.

The phenomenological parametrization scheme works well for the dynamic IF of soft ferromagnetic metals with a cubic lattice structure. The tolerance of fitting is 0.01×10^{-3}. The parameters c_i ($i = 1, 2$) are associated, respectively, with the percentage of moving and stopped DWs in ΔH and $c_1 > c_2$ in general holds to produce the dynamic IF (fitted from the effective zero H). Thus, c_i are called the DW initial distribution parameters. In annealed samples, c_i increase with increasing $\dot{H}$ but this tendency is reversed for pre-strained samples. c_i also increase with increasing ω in annealed Fe and Permalloy-42. These variations show the effect of processing on the internal stress, the defect distribution, the sizes of the DWs and, in particular, the DW mobility. The parameters b_i are called the decay constants and they do not show a distinct tendency with the sweeping rate. The fitted results show that b_1 and b_2 are different in general so that the moving and stopping mechanisms should be different and it is impossible to reduce the two-term expression into a one-term exponent form (we did initially attempt to do this). The dynamic IF increases with increasing sweeping rate, and hence the area under the Q_m^{-1} versus H curve, which can be interpreted as the total dissipated dynamic energy due to the resistance to DW motion, also increases. The total dissipated dynamic energy, denoted as Q_V, is readily obtained as

$$Q_V = \int_0^\infty Q_m^{-1}\, dH = \frac{c_1 b_2 - c_2 b_1}{b_1 b_2} \tag{13}$$

based on equation (12) and also

$$Q_V = (a_2 l/a_1)(E\dot{H}/M_s\omega) \text{ or } [(a_2 l/a_1)(kE/M_s)]\dot{H}^s/\omega^{1+s-2\alpha} \tag{14}$$

based on equation (11) or (11*). We shall apply the values obtained from equation (13) to fit the index parameters α and s, which are expected to be smaller than unity, and to test the linearity of Q_V versus $\dot{H}/\omega$ and Q_V versus $\dot{H}^s/\omega^{1+s-2\alpha}$ instead of Q_m^{-1} versus $\dot{H}/\omega$ as in figure 6 of I.

Figure 2 shows the curves of Q_V versus $\dot{H}/\omega$ for Fe, Permalloy and Ni and they are essentially not linear. Figure 3 shows the lines of Q_V versus $\dot{H}^s/\omega^{1+s-2\alpha}$ for the three soft ferromagnetic materials. The index parameters are given in table 3. The α-values of Fe and Permalloy are first determined from Q_0^{-1} based on equation (9*). Their consistency can also be shown by considering the ratios of the slopes of the lines in figure 3. The modulus E and the orientation factor a_1 are not sensitive to structure and the a_2- and l-values are assumed to be the same for all three metals. Hence, considering their very close values of modulus (e.g. Young's moduli of 211.4 GPa and 199.5 GPa for soft iron and Ni, respectively; shear moduli of 81.6 GPa and 76.0 GPa for soft Fe and Ni, respectively), the coefficients in front of $\dot{H}^s/\omega^{1+s-2\alpha}$ can be taken approximately the same for these metals and the slope ratio will provide an estimate of the relative ratio of their saturation magnetization M_s. We obtain M_s(Ni): M_s(Permalloy): M_s(Fe) = 1:2:4. The ratios are reasonable when compared with the classical values of M_s: 0.6 T, 1.2 T

Table 2. Parameters c_1, c_2, b_1 and b_2 for Q_m^{-1} (equation (12)), Q_V and $\dot{H}/\omega$.

Sample	Strain amplitude $\times 10^6$	Frequency (Hz)	$\dot{H}$ (mOe s^{-1})	$c_1 \times 10^3$	$c_2 \times 10^3$	b_1 (Oe^{-1})	b_2 (Oe^{-1})	$Q_V \times 10^3$	$\dot{H}/\omega$ (mOe)
Fe	4.5	1.100	8.5	0.75	0.59	0.2860	2.906	2.43	1.23
Fe	4.5	1.100	23.5	1.93	1.93	0.3489	1.618	4.34	3.40
Fe	4.5	1.100	39.5	1.97	1.45	0.2824	2.191	6.36	5.72
Fe	4.5	1.100	66.5	2.44	1.15	0.2536	1.835	9.00	9.62
Fe	4.5	1.600	8.7	271.44	271.32	0.9060	0.9087	1.02	0.865
Pre-strained Fe	4.5	1.600	21.3	2139.02	2138.78	0.7618	0.7623	2.16	2.12
Pre-strained Fe	4.5	1.100	9.2	162.02	161.74	0.4737	0.4757	2.03	1.33
Pre-strained Fe	4.5	1.100	39.8	269.11	295.47	0.4617	0.4644	5.11	5.76
	4.5	1.100	66.2	2.73	2.17	0.2736	0.8838	7.53	9.58
Ni	10	1.013	10.0	2.56	2.04	0.4454	5.052	5.35	1.57
Ni	10	1.013	20.0	7.69	5.42	0.4405	1.418	13.64	3.14
Ni	10	1.013	40.0	10.50	6.91	0.3253	2.143	29.04	6.29
Ni	10	1.013	80.0	14.21	3.65	0.2713	2.143	50.67	12.57
Ni	10	1.330	10.0	2.57	1.84	0.4281	1.105	4.33	1.20
Ni	10	1.330	20.0	4.05	2.66	0.3022	1.367	11.45	2.39
Ni	10	1.330	40.0	8.79	5.56	0.2805	0.7784	24.20	4.79
Ni	10	1.330	80.0	530.12	525.02	0.3924	0.3996	37.11	9.57
Pre-strained Ni	10	1.014	10.0	293.50	293.34	0.6784	0.6822	2.63	1.57
Pre-strained Ni	10	1.014	20.0	5.37	5.26	0.3984	0.8159	7.03	3.14
Pre-strained Ni	10	1.014	40.0	3.88	3.46	0.2343	1.062	13.30	6.28
Pre-strained Ni	10	1.014	80.0	3.97	3.93	0.1569	1.412	22.53	12.56
Permalloy	50	0.773	20.0	1.26	0.87	0.1762	0.5421	5.53	4.12
Permalloy	50	0.773	40.0	1.47	0.83	0.1451	0.7803	8.97	8.24
Permalloy	50	0.773	80.0	1.83	1.62	0.1356	1.225	12.21	16.47
Permalloy	50	1.586	20.0	86.47	86.42	0.3210	0.3224	1.32	2.01
Permalloy	50	1.586	40.0	70.39	70.10	0.3238	0.3269	2.95	4.01
Permalloy	50	1.586	80.0	1366.06	1365.65	0.3473	0.3476	4.75	8.03

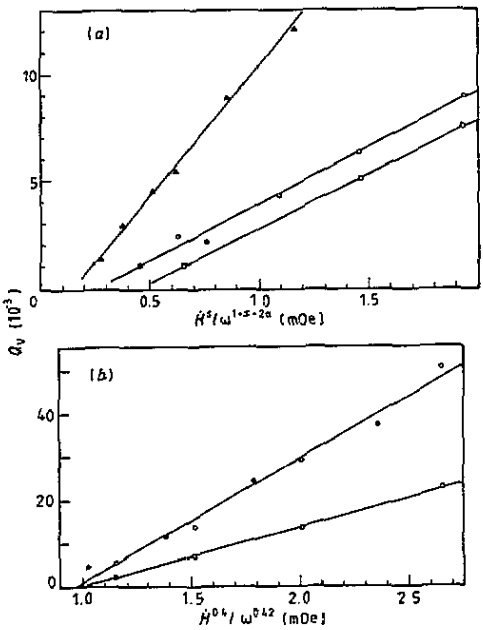

Figure 3. The total dissipated dynamic energy Q_V versus $\dot{H}^s/\omega^{1+s-2\alpha}$ (*a*) of Fe with $s = 0.55$ and $\alpha = 0.35$ and Permalloy with $s = 0.45$ and $\alpha = 0.15$ (○, annealed Fe at $f = 1.100$ Hz; ●, annealed Fe at $f = 1.600$ Hz; □, pre-strained Fe at $f = 1.100$ Hz; △, annealed Permalloy at $f = 0.773$ Hz; ▲, annealed Permalloy at $f = 1.586$ Hz) and (*b*) of Ni with $s = 0.40$ and $\alpha = 0.49$ (○, annealed Ni at $f = 1.013$ Hz; ●, annealed Ni at $f = 1.330$ Hz; □, pre-strained Ni at $f = 1.014$ Hz).

Table 3. Index parameters for Fe, Permalloy and Ni.

	Fe	Permalloy	Ni
α	0.35	0.15	0.49
s	0.55	0.45	0.40

and 2.1 T for nickel, Permalloy and Fe, respectively (Cullity 1972). In the case of cold-worked samples, a_2 decreases with cold working as the magnetostriction factor decreases. Therefore the slopes for the annealed materials are larger than those of the cold-worked materials. It is notable in the Ni case but not so in the Fe case since Fe is a pinning material and its DWs are already pinned by interstitial impurities. On the other hand, the α- and s-values for Permalloy are not in between those for Fe and Ni, which shows the coupling of the applied stress to DWs and that the DW motion in Permalloy is different from those in Fe and Ni since the DW motion of Permalloy is not that of a simple mixture of these two kinds of DW.

The static IF behaves differently for different materials as shown in figures 3–5 of I. The static IF of Fe and Permalloy increases with increasing frequency and can be interpreted from equation (9*). However, the Q_0^{-1} for Ni changes in the opposite

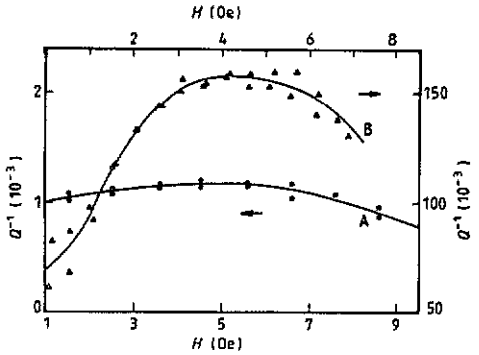

Figure 4. The normalized curves of Q_0^{-1} versus H: curve A, Permalloy (○, at $f = 0.733$ Hz; ●, at $f = 1.589$ Hz) left ordinate; curve B, annealed Ni (△, at $f = 1.013$ Hz; ▲, at $f = 1.330$ Hz) right ordinate.

direction. Curve (A) in figure 4 is a normalized curve of Q_0^{-1} versus H which is obtained from curves with different strain frequencies by multiplying by a factor of $(\omega^{1-2\alpha})^{-1}$. The scale of Q_0^{-1} is kept the same as figure 5 of I and the agreement is reasonably good. In contrast, the static IF of annealed Ni as shown by curve (B) is normalized by multiplying by a factor of $\omega^{1.82}$ whose index is not related to the α-value of annealed nickel (0.5). It shows that the Q_0^{-1} for annealed Ni originates from mechanisms different from that associated with equation (9*). When the magnetic field is increased in a stepwise manner and the IF is measured at each new constant field value by applying an alternating strain, the DWs of the pinning materials such as Fe, Permalloy and cold-worked Ni only oscillate about a new equilibrium position because they are pinned, but time-dependent depinning processes occur for materials with weak pinning and few pinning centres even at room temperature, which causes additional IF. The longer the measurement period is (the smaller the frequency ω), the larger the depinning chance will be. So a larger static IF results. This is the case for annealed Ni. Even at room temperature, the static IF of annealed Ni decreases with increase in the strain frequency.

It is possible to clarify the physical significance of the rate-sensitive indices by investigating the phenomena which are related to interface motion such as the plastic deformation of polycrystalline Al and the martensitic phase transition of NiTi shape memory alloy where both the field sweep rate and the frequency of the applied strain are varied over a large range.

4. Summary

Soft ferromagnetic metals with a cubic lattice structure—pure iron, nickel and Permalloy-42—all show similar dynamic behaviour in low-frequency anelastic studies when they are magnetized. An interaction model is proposed to study the DW motion in a uniformly increasing magnetic field with an alternating stress. The solutions show that the dynamic IF is of a viscoelastic type and increases as $\dot{H}^s/\omega^{1+s-2\alpha}$. The dynamic IF results from the magnetomechanical interaction and is a characteristic of this coupling force. Its form is consistent with the results of interface dynamics. Furthermore, dynamic IF data are fitted by a four-parameter phenomenological model and lead to an interpretation of DW motion. This is achieved by the results of the interaction model which

show that the dynamic IF is connected with the magnetization of the soft ferromagnetic metals. To clarify the relationship between the two, the experimental data on differential susceptibility as a function of magnetic field should be obtained. We leave this problem for further study.

References

Bertotti G 1987 *Proc. 3rd Int. Conf. on the Physics of Magnetic Materials* (Singapore: World Science) pp 489–508

Cullity B D 1972 *Introduction to Magnetic Materials* (Reading, MA: Addison-Wesley)

Degauque J and Astié B 1980 *Phys. Status Solidi* a **59** 805–16

Ké T S and Zhang J X 1975 *Acta Phys. Sin.* **24** 87–90

Kittel C and Galt J K 1956 *Solid State Physics* vol 3 (New York: Academic) pp 437–564

Lin Z C, Liang K F, Zeng W G and Zhang J X 1989 *Internal Friction and Ultrasonic Attentuation* ed T S Ké and L D Zhang (Peking: Atomic Energy Press) pp 87–8

O'Dell T H 1981 *Ferromagnetodynamics* (New York: Wiley) ch 1

Peking University (Department of Physics) 1976 *Ferromagnetism* (Peking: Science)

Zeng W G, Lin H Q, Zhang J X and Siu G G 1990 *J. Phys.: Condens. Matter* **2** 9531–9

Zhang J X 1981 *J. Physique* **42** 399